



Scholars Research Library

Der Pharmacia Lettre, 2013, 5 (2):27-39  
(<http://scholarsresearchlibrary.com/archive.html>)



## Experimental investigation and theoretical approach on water soluble acridin derivative as corrosion inhibitor

A. H. Al Hamzi<sup>1</sup>, H. Zarrok<sup>2</sup>, A. Zarrouk<sup>3,\*</sup>, R. Salghi<sup>5</sup>, B. Hammouti<sup>3</sup>, M. Bouachrine<sup>4</sup>, A. Amine<sup>1</sup>, F. Guenoun<sup>1</sup> and H. Oudda<sup>2</sup>

<sup>1</sup>Laboratoire Chimie – Biologie Appliquées à l'Environnement, Equipe CMMBA, Université Moulay Ismail, Faculté des Sciences, Meknès, Morocco

<sup>2</sup>Laboratoire des procédés de séparation, Faculté des Sciences, Université Ibn Tofail, Kénitra, Morocco

<sup>3</sup>LCAE-URAC18, Faculté des Sciences, Université Mohammed I<sup>er</sup>, Oujda, Morocco

<sup>4</sup>ESTM, Université Moulay Ismail, Meknes, Morocco

<sup>5</sup>Equipe de Génie de l'Environnement et Biotechnologie, ENSA, Université Ibn Zohr, BP1136 Agadir, Morocco

### ABSTRACT

The effect of 2-methylacridin-9(10H)-one (MAO) on the corrosion of carbon steel in aqueous solution of 1.0 M hydrochloric acid was investigated at different 308K by weight loss, electrochemical techniques and theoretical quantum chemical calculations data indicated that their inhibition effect are closely related to  $E_{HOMO}$ ,  $E_{LUMO}$ , hardness, dipole moment and charge densities. The results obtained showed that MAO could serve as an effective inhibitor for the corrosion of carbon steel in hydrochloric acid media. The results indicated that an increase in the inhibitor concentration leads to an increase in both the charge-transfer resistance ( $R_{ct}$ ) and inhibition efficiency (IE) and to a decrease of the corrosion current density ( $I_{corr}$ ). The inhibitive mechanism was discussed assuming the adsorption of MAO on the electrode surface. Theoretical fitting of different isotherms, Langmuir, Flory-Huggins, and the kinetic-thermodynamic models, were tested to clarify the nature of adsorption.

**Keywords:** Acid inhibitor, Carbon steel, EIS, Polarization, Quantum chemical calculations.

### INTRODUCTION

Mild steel as an important construction material is extensively used in all kinds of industry and corrosion of mild steel known to occur especially in acid environment such as cleaning, pickling, oil well acidification and descaling processes [1-5]. It is a major task to control the mild steel corrosion for both corrosion scientist and material technologist. Several methods are employed to prevent mild steel from corrosion but addition of inhibitors has been known to be the most effective method for its practical application [6-9]. A large number of studies about various types of organic inhibitors have been previously reported [10-30]. Organic molecules can form a barrier through adsorption on the metal surface to reduce the corrosion of metal in acidic solution [31,32]. So most of efficient inhibitors are organic compounds in their structures containing heteroatoms (such as, N, S, P and O) donating lone pair electrons, unsaturated bonds (such as double bonds, or triple bonds), and plane conjugated systems including all kinds of aromatic cycles [33-38]. It has been observed that the adsorption depends mainly on the electronic and structural properties of the inhibitor molecule such as functional groups, steric factors, aromaticity, electron density on donor atoms and  $\pi$  orbital character of donating electrons [39-41]. The geometry of the inhibitor in its ground state, as well as the nature of their molecular orbitals, HOMO (highest occupied molecular orbital) and LUMO (lowest unoccupied molecular orbital) are involved in the properties of inhibitors activity. Quantum chemistry calculations have been widely used to study the reaction mechanisms and to interpret the experimental results [42,43]. The structure and electronic parameters can be obtained by means of theoretical calculation using the

computational methodologies of quantum chemistry [44,45]. Quantum Chemical calculations have become an effective method to study the correlation of the molecular structure and its inhibition properties [46,47].

In continuation of work on the acid corrosion inhibitors, 2-methylacridin-9(10H)-one (MAO) was used as a corrosion inhibitor for carbon steel in 1.0 M HCl solution. The investigation is performed using weight loss measurements, electrochemical methods and electrochemical impedance spectroscopy (EIS) measurements. The work will extend to find a correlation between the inhibition efficiency and the electronic properties of the studied molecules. The chemical structure of the studied MAO derivative is given in Fig 1.

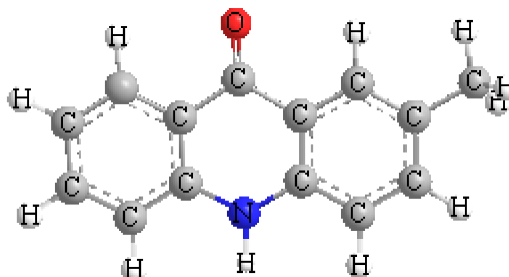


Figure 1. The chemical structure of the studied acridin derivative compound.

## MATERIALS AND METHODS

### Materials

The steel used in this study is a carbon steel (CS) (Euronorm: C35E carbon steel and US specification: SAE 1035) with a chemical composition (in wt%) of 0.370 % C, 0.230 % Si, 0.680 % Mn, 0.016 % S, 0.077 % Cr, 0.011 % Ti, 0.059 % Ni, 0.009 % Co, 0.160 % Cu and the remainder iron (Fe).

### Solutions

The aggressive solutions of 1.0 M HCl were prepared by dilution of analytical grade 37% HCl with distilled water. The organic compound tested is 2-methylacridin-9(10H)-one (MAO). The concentration range of this compound was  $10^{-3}$  to  $10^{-6}$  M.

### Weight loss measurements

Coupons were cut into  $2 \times 2 \times 0.08$  cm<sup>3</sup> dimensions are used for weight loss measurements. Prior to all measurements, the exposed area was mechanically abraded with 180, 320, 800, 1200 grades of emery papers. The specimens were washed thoroughly with bidistilled water, degreased and dried with ethanol. Gravimetric measurements are carried out in a double walled glass cell equipped with a thermostated cooling condenser. The solution volume is 50 mL. The immersion time for the weight loss is 6 h at 308 K. In order to get good reproducibility, parallel triplicate experiments were performed and the average weight loss value of three parallel carbon steel sheets was obtained. The corrosion rate ( $v$ ) was calculated by the following equation:

$$v = \frac{w}{St} \quad (1)$$

Where  $v$  was the corrosion rate in (mg cm<sup>-2</sup> h<sup>-1</sup>),  $w$  is the average weight loss of three parallel carbon steel sheets (mg),  $S$  was the total area of one carbon steel sheet (cm<sup>2</sup>), and  $t$  was immersion time (h).

With the calculated corrosion rate, the inhibition efficiency ( $\eta_{WL}$  %) was obtained as the following equation:

$$\eta_{WL} \% = \frac{v_0 - v}{v_0} \times 100 \quad (2)$$

Where  $v_0$  and  $v$  are the values of corrosion rate without and with different concentration of inhibitor, respectively.

### Polarization measurements

#### Electrochemical impedance spectroscopy

The electrochemical measurements were carried out using Volta lab (Tacussel- Radiometer PGZ 100) potentiostat and controlled by Tacussel corrosion analysis software model (Voltmaster 4) at under static condition. The corrosion cell used had three electrodes. The reference electrode was a saturated calomel electrode (SCE). A

platinum electrode was used as auxiliary electrode of surface area of 0.094 cm<sup>2</sup>. The working electrode was carbon steel. All potentials given in this study were referred to this reference electrode. The working electrode was immersed in test solution for 30 minutes to establish steady state open circuit potential ( $E_{ocp}$ ). After measuring the  $E_{ocp}$ , the electrochemical measurements were performed. All electrochemical tests have been performed in aerated solutions at 308 K. The EIS experiments were conducted in the frequency range with high limit of 100 kHz and different low limit 0.1 Hz at open circuit potential, with 10 points per decade, at the rest potential, after 30 min of acid immersion, by applying 10 mV ac voltage peak-to-peak. Nyquist plots were made from these experiments. The best semicircle can be fit through the data points in the Nyquist plot using a non-linear least square fit so as to give the intersections with the  $x$ -axis.

The inhibition efficiency of the inhibitor was calculated from the charge transfer resistance values using the following equation [48]:

$$\eta_z \% = \frac{R_{ct(inh)} - R_{ct}}{R_{ct(inh)}} \times 100 \quad (3)$$

where  $R_{ct}$  and  $R_{ct(inh)}$  were the values of polarization resistance in the absence and presence of inhibitor, respectively.

### Potentiodynamic polarization

The electrochemical behaviour of carbon steel sample in inhibited and uninhibited solution was studied by recording anodic and cathodic potentiodynamic polarization curves. Measurements were performed in the 1.0 M HCl solution containing different concentrations of the tested inhibitor by changing the electrode potential automatically from -800 to -200 mV versus corrosion potential at a scan rate of 1 mV s<sup>-1</sup>. The linear Tafel segments of anodic and cathodic curves were extrapolated to corrosion potential to obtain corrosion current densities ( $I_{corr}$ ). From the polarization curves obtained, the corrosion current ( $I_{corr}$ ) was calculated by curve fitting using the equation:

$$I = I_{corr} \left[ \exp\left(\frac{2.3\Delta E}{\beta_a}\right) - \exp\left(\frac{2.3\Delta E}{\beta_c}\right) \right] \quad (4)$$

The inhibition efficiency was evaluated from the measured  $I_{corr}$  values using the relationship:

$$\eta_{Tafel} \% = \frac{I_{corr}^{\circ} - I_{corr}^i}{I_{corr}^{\circ}} \times 100 \quad (5)$$

where,  $I_{corr}^{\circ}$  and  $I_{corr}^i$  are the corrosion current density in absence and presence of inhibitor, respectively.

### Computational details

Density functional theory (DFT) calculations were carried out using the Becke three-parameter nonlocal exchange functional [49] with the nonlocal correlation of Lee et al. [50] and Miehlich et al. [51], together with the standard double-zeta plus polarization 6-31G(d,p) basis set [52] implemented in the GAUSSIAN 03 program package [53]. Following the standard nomenclature the calculation will be referred to as B3LYP/6-31G\*. The geometry of this compound under investigation was determined by optimizing all geometrical variables without any symmetry constraints.

According to DFT-Koopmans' theorem [54-56], the ionization potential  $I$  can be approximated as the negative of the highest occupied molecular orbital (HOMO) energy,

$$I = -E_{HOMO} \quad (6)$$

The negative of the lowest unoccupied molecular orbital (LUMO) energy is similarly related to the electron affinity  $A$ ,

$$A = -E_{LUMO} \quad (7)$$

The obtained values of  $I$  and  $A$  were considered for the calculation [57] of the electronegativity  $\chi$  and the global hardness  $\eta$  in each of the tested molecule using the following relations:

$$\chi = \frac{I + A}{2} \quad (8)$$

$$\eta = \frac{I - A}{2} \quad (9)$$

During the interaction of the inhibitor molecule with bulk metal, electrons flow from the lower electronegativity molecule to the higher electronegativity metal until the chemical potential becomes equalized. The fraction of the transferred electron,  $\Delta N$ , was estimated according to Pearson [57]

$$\Delta N = \frac{\chi_{Fe} - \chi_{inh}}{2(\eta_{Fe} + \eta_{inh})} \quad (10)$$

where a theoretical value for the electronegativity of bulk iron was used,  $\chi(Fe) = 7$  eV, and a global hardness of  $\eta(Fe) = 0$  was used [58].

## RESULTS AND DISCUSSION

### Electrochemical Impedance Spectroscopy (EIS)

Fig. 2 shows the Nyquist plots of carbon steel at the corrosion potentials in 1.0 M HCl solution with addition of different concentration of MAO. The characteristic of a single semicircle shows the existence of single charge transfer process during carbon steel dissolution which is unaffected by MAO molecules. The slightly depressed capacitive loop which has the center below the x-axis is the representation for solid electrodes and the frequency dispersion has been ascribed to the inhomogenities of the solid electrode [59, 60]. The solution resistance ( $R_s$ ), the charge transfer resistance ( $R_{ct}$ ), the interfacial double layer capacitance ( $C_{dl}$ ) values derived from these plots and the calculated inhibition efficiency ( $\eta_z\%$ ) according to equation (3) are given in Table 1.

**Table 1. Electrochemical impedance parameters and inhibition efficiency for carbon steel in 1.0 M HCl solution with MAO at 308K.**

	Conc (M)	$R_s$ ( $\Omega$ cm <sup>2</sup> )	$R_{ct}$ ( $\Omega$ cm <sup>2</sup> )	$f_{max}$ (Hz)	$C_{dl}$ ( $\mu$ F/cm <sup>2</sup> )	$\eta_z$ (%)
Blank	1.0	1.67	31.04	63.34	80.99	-
	$10^{-3}$	1.30	533.70	12.50	23.85	94.2
MAO	$10^{-4}$	1.36	367.89	15.82	27.34	91.6
	$10^{-5}$	1.45	190.25	20.00	41.82	83.7
	$10^{-6}$	1.60	153.26	25.00	41.53	79.7

For corrosion reactions which are strictly charge transfer controlled, impedance behaviour can be explained with the help of a simple and commonly used equivalent circuit which composed of a double layer capacitance,  $R_{ct}$  and  $R_s$ . The resistor  $R_s$  is in series to the double layer capacitance and  $R_{ct}$  while double layer capacitance is parallel to  $R_{ct}$ . The double layer capacity is in parallel with the impedance due to the charge transfer reaction. This type of circuit has been used previously to model the iron-acid interface [61, 62]. The constant phase element, CPE, is introduced in the circuit instead of a pure double layer capacitance to give more accurate fit as shown in the Fig. 3 [63].

It is clear that the addition of MAO increases the value of  $R_{ct}$  from the value of 31.04  $\Omega$  cm<sup>2</sup> (blank) to 533.7  $\Omega$  cm<sup>2</sup> (1.0 mM MAO) and this in turn leads to an increase in the inhibition efficiency from 79.74% to 94.20% ( $10^{-3}$ - $10^{-6}$ M MAO). On the other hand, the addition of MAO lowers the  $C_{dl}$  value from 41.53 to 23.85  $\mu$ F cm<sup>-2</sup>. Decrease in  $C_{dl}$ , which is due to a decrease in local dielectric constant and/or an increase in the thickness of the electrical double layer, suggests that the MAO function by adsorption at the carbon steel-solution interface [64].

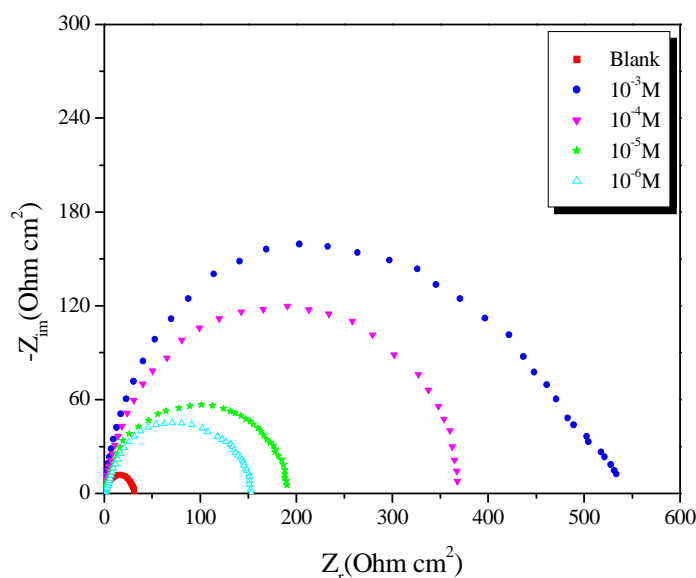


Figure 2. Nyquist plots for carbon steel in 1.0 M HCl solution in presence of various concentrations of MAO at 308K.

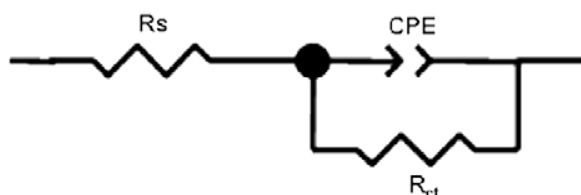


Figure 3. The equivalent circuit.

### Potentiodynamic polarization curves

Fig. 4 show potentiodynamic polarization curves for carbon steel in 1.0 M HCl solutions without and with various concentrations of this compound. The electrochemical kinetic parameters, i.e., corrosion current densities ( $I_{corr}$ ), corrosion potential ( $E_{corr}$ ) and cathodic Tafel slope ( $\beta_c$ ) are presented in Table 2. The inhibition efficiency ( $\eta_{Tafel}$ ) of the used extract in 1.0 M HCl is also given in Table 2.

$E_{corr}$  values slightly shifted toward both positive and negative direction in the presence of different concentrations of acridin derivative in 1.0 M HCl. If the shift of the  $E_{corr}$  values in the presence of corrosion inhibitor is greater than 85 mV, the compound is an inhibitor of anodic type and vice versa, i. e. if the shift is lower than 85 mV, the inhibitor belongs to the cathodic type [65]. Therefore, compound evaluated as corrosion inhibitor is usually classified as mixed type inhibitor. However, it is clearly observed from Fig.4 that the inhibitor reduces the anodic and cathodic current densities, indicating the inhibition effects of this compound. Cathodic polarization curves also show parallel lines with the inhibitor concentration with respect to the polarization curve of the blank. This behavior in the cathodic process, suggests that the addition of the corrosion inhibitor in the corrosive medium does not modify the mechanism of reduction of protons, and that the reaction is only controlled by the activation energy. This also suggests that once the inhibitor compound is adsorbed on the metal surface, it blocks off the active sites. Under these circumstances, the available metal surface ( $1-\theta$ ) for free  $H^+$  ions is reduced, while the reaction mechanism is not affected [66, 67].

In addition, from Table 2, the slope of the cathodic Tafel lines ( $\beta_c$ ) are observed to slightly change by the addition of the inhibitor, the small change may be due to surface blockage by MAO. The data in Table 2 apparently showed that, the corrosion current densities decreased with increasing the inhibitor concentrations and the inhibition efficiencies increased.

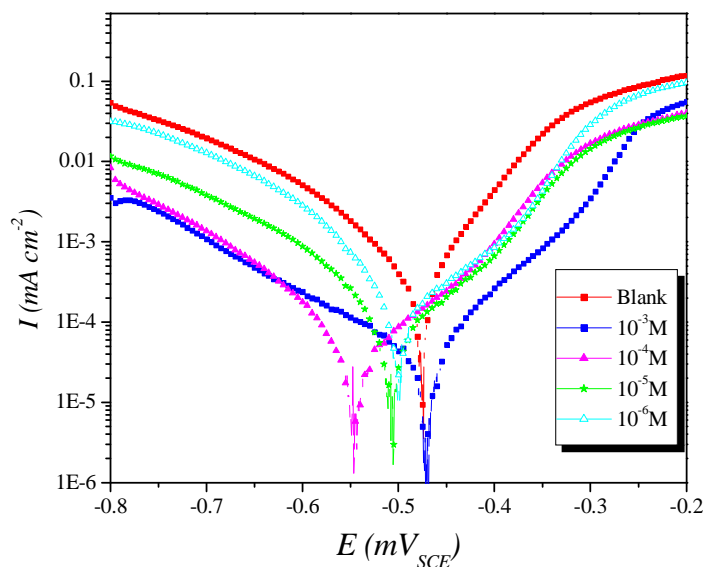


Figure 4. Polarisation curves of carbon steel in 1.0 M HCl for various concentrations of MAO.

Table 2. Polarisation data of carbon steel in 1.0 M HCl without and with addition of inhibitor at 308 K.

Inhibitor	Conc (M)	$-E_{\text{corr}}$ (mV/SCE)	$-\beta_c$ (mV/dec)	$I_{\text{corr}}$ ( $\mu\text{A cm}^{-2}$ )	$\eta_{\text{Tafel}}$ (%)
Blank	1.0	475.9	175.6	1077.8	----
MAO	$10^{-3}$	473.1	182.8	48.10	95.6
	$10^{-4}$	548.1	153.4	106.6	90.1
	$10^{-5}$	510.1	150.4	176.6	83.6
	$10^{-6}$	508.1	164.6	219.4	79.6

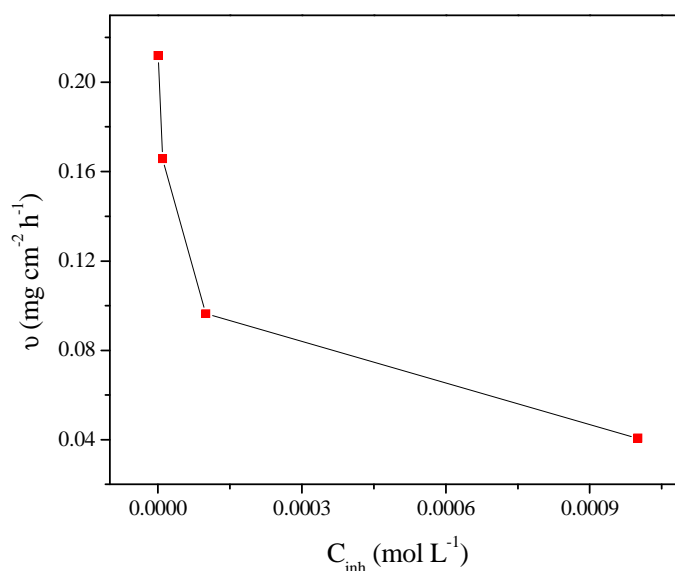


Figure 5. Relationship between corrosion rate ( $v$ ) and concentration of MAO in 1.0 M HCl solutions at 308 K.

#### Weight loss tests

The weight loss method of monitoring corrosion rate and inhibition efficiency is useful owing to its simple application and good reliability [68-69]. Fig. 5 shows the corrosion rate ( $v$ ) values of carbon steel in 1.0 M HCl

solutions without and with different concentrations of MAO at 308K. In acidic media, it is obvious that the MAO effectively inhibits the corrosion rate of carbon steel in HCl media. Corrosion rate  $v$  decreases noticeably with an increase in MAO concentration.

At the maximum concentration of  $10^{-3}$  M MAO, the corrosion rate value from  $0.041 \text{ mg cm}^{-2} \text{ h}^{-1}$  is decreased to  $0.212 \text{ cm}^{-2} \text{ h}^{-1}$  in 1.0 M HCl solutions. This behavior is due to the fact that the adsorption amount and coverage of inhibitor on carbon steel surface increase with the inhibitor concentration [70].

The variation in inhibition efficiency with concentration of MAO obtained from weight loss measurement at 308 K is shown in Fig.6. From Fig.6, it is clear the  $\eta_{WL}\%$  increases with an increase in concentration and exhibits the opposite variation compared to corrosion rate in 1.0 M HCl solutions. The increase in inhibition efficiency is due to the increase in the number of MAO adsorbed on the carbon steel surface at higher concentrations, so that the active sites of the metal are protected by MAO molecules. The maximum  $\eta_{WL}\%$  value is 96.2% 0.5 M at  $10^{-3}$  M concentration which indicates that MAO is a very good inhibitor for carbon steel in HCl and solutions.

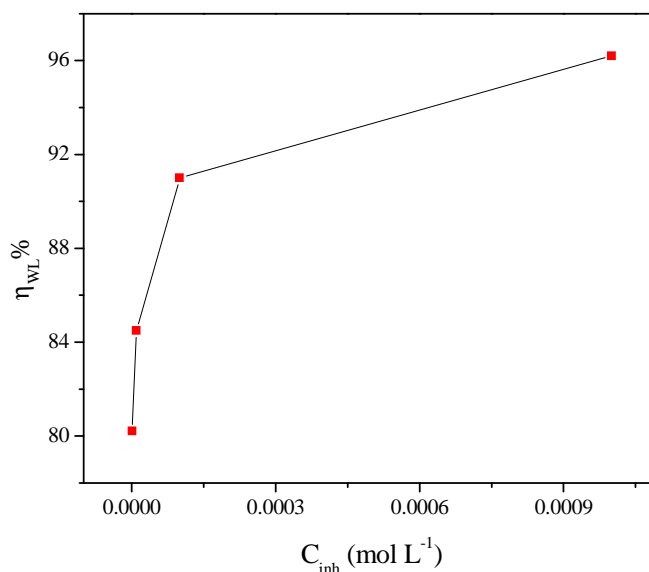


**Figure 6. Relationship between inhibition efficiency ( $\eta_{WL}\%$ ) obtained from weight loss measurements and concentration of MAO in 1.0 M HCl solutions at 308K.**

#### Application of adsorption isotherms

Basic information on the interaction between inhibitor and steel surface can be provided by adsorption isotherm. The degree of surface coverage ( $\theta$ ) of the metal surface by an adsorbed inhibitor molecule is calculated from impedance measurements using the equation:

$$\theta = \frac{v_0 - v}{v_0} \quad (11)$$

The Langmuir isotherm is given by [71]:

$$\left[ \frac{\theta}{(1-\theta)} \right] = KC \quad (12)$$

where K is the binding constant representing the interaction of the additives with metal surface and C is the concentration of the additives.

Flory-Huggins isotherm is given by [72, 73]:

$$\theta / \left[ x(1-\theta)^x \right] = KC \quad (13)$$

where  $x$  is the size parameter and is a measure of the number of adsorbed water molecules substituted by a given inhibitor molecule.

and the kinetic-thermodynamic model is given by [74]:

$$\text{Ln}\left[\frac{\theta}{1-\theta}\right] = \text{Ln}K' + y\text{Ln}C \quad (14)$$

where  $y$  is the number of inhibitor molecules occupying one active site. The binding constant  $K$  is given by

$$K = K'^{(1/y)} \quad (15)$$

Figures (7-9) show the application of the above mentioned models to fit the corrosion data of the inhibitor.

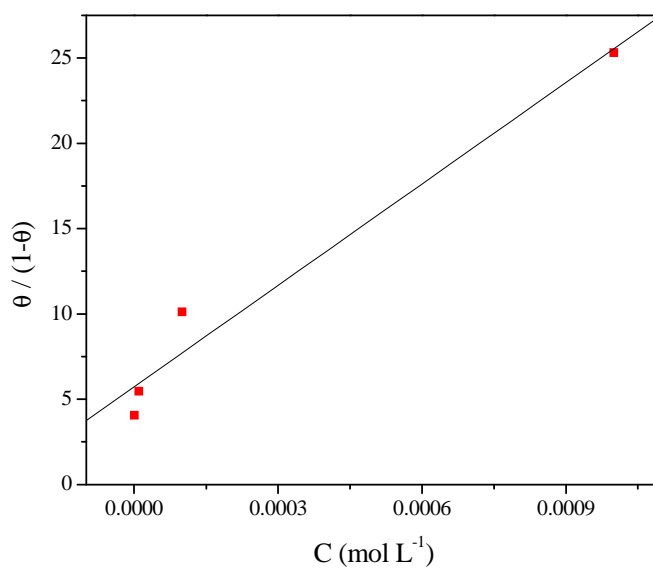


Figure 7. Linear square fit of weight loss data to Langmuir isotherm.

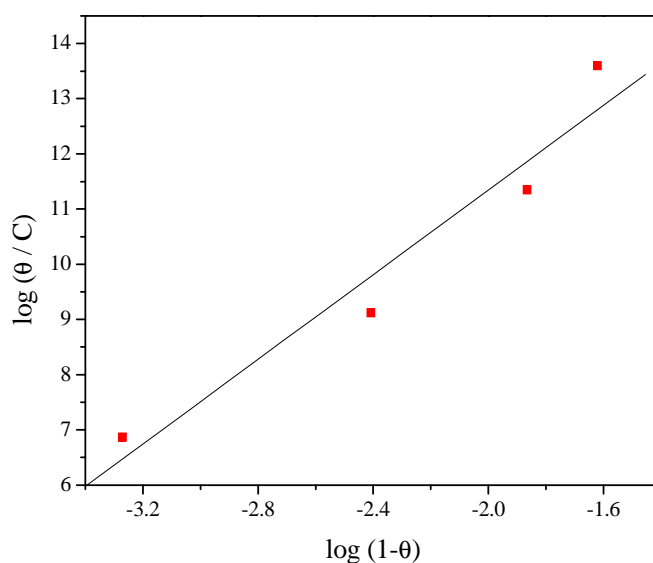


Figure 8. Linear square fit of weight loss data to Flory Huggins isotherm.

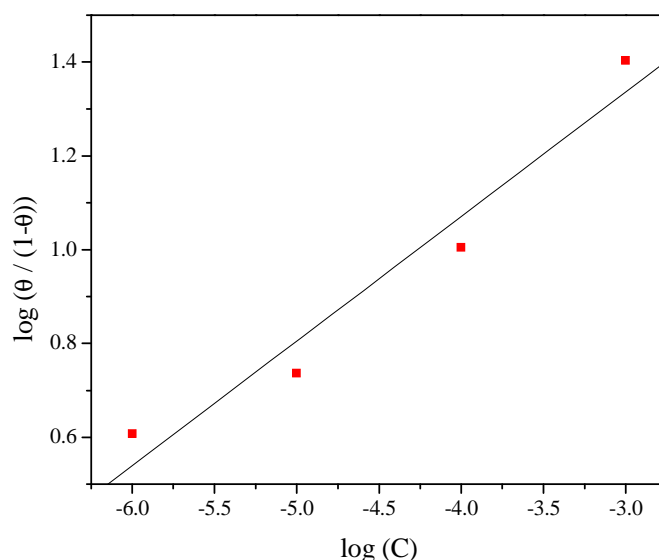


Figure 9. Linear square fit of weight loss data to Kinetic-Thermodynamic model.

The parameters obtained from these Figures are given in Table 3. The parameters reveal that Langmuir isotherm is applicable to fit the corrosion data of MAO indicating an ideal behavior in the adsorption processes on the steel surface [75]. The value of the size parameter  $x$  indicates that the adsorbed species of MAO could displace four water molecules from the steel surface. The number of active sites occupied by a single inhibitor molecule,  $1/y$ , are nearly equal to the size parameter  $x$ . The  $1/y$  value indicates that the adsorbed molecules cover four active centers. The binding constant values ( $K$ ) show a fairly good agreement between Langmuir and Flory-Huggins isotherm but not with the Kinetic thermodynamic model.

Table 3. Linear fitting parameters of Langmuir, Flory-Huggins and Kinetic-thermodynamic model for MAO at 308K.

Langmuir		Flory Huggins			Kinetic-Thermodynamic		
K	$\Delta G_{ads}^{\circ}$ (kJ/mo)	x	K	$\Delta G_{ads}^{\circ}$ (kJ/mo)	1/y	K	$\Delta G_{ads}^{\circ}$ (kJ/mo)
19823.26	-35.62	3.8347	20503.7	-35.71	3.7652	107646507.48	-57.64

The values of the Gibbs free energy of adsorption ( $\Delta G_{ads}^{\circ}$ ) calculated from the equation [76]:

$$\Delta G_{ads}^{\circ} = -RTL \ln(55.5 K_{ads}) \quad (16)$$

where  $R$  is gas constant and  $T$  is absolute temperature of experiment and the constant value of 55.5 is the concentration of water in solution in  $\text{mol L}^{-1}$ .

The negative values of  $\Delta G_{ads}^{\circ}$  calculated from Eq. (16), are consistent with the spontaneity of the adsorption process and the stability of the adsorbed layer on the carbon steel surface. Generally, values of  $\Delta G_{ads}^{\circ}$  up to  $-20 \text{ kJ mol}^{-1}$  are consistent with physisorption, while those around  $-40 \text{ kJ mol}^{-1}$  or higher are associated with chemisorption as a result of the sharing or transfer of electrons from organic molecules to the metal surface to form a coordinate bond [77]. The calculated  $\Delta G_{ads}^{\circ}$  values with Langmuir and Flory-Huggins show, therefore, that the adsorption mechanism of this compound on steel involves both two types of interaction. Indeed, due to the strong adsorption of water molecules on the surface of carbon steel, one may assume that adsorption occurs first due to the physical force. The removal of water molecules from the surface is accompanied by chemical interaction between the metal surface and adsorbate, and that turns to chemisorptions [78]. In sum, the large negative values of  $\Delta G_{ads}^{\circ}$  reveal that the adsorption process takes place spontaneously and the adsorbed layer on the surface of carbon steel is highly stable [79].

### Quantum chemical calculations

Recently, theoretical prediction of the efficiency of corrosion inhibitors using quantum chemical calculations has become very popular in parallel with the progress in computational hardware and the development of efficient algorithms [10,32]. All quantum DFT calculated parameters were obtained after geometric study by optimization of the structure of each studied compound with *DFT/B3LYP/6-31G\*(d) method*. The obtained optimized structure of the studied compound is shown in Fig. 10.

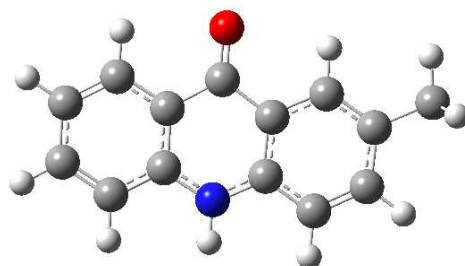


Figure 10. Optimized structure of MAO obtained by B3LYP/6-31G\* level

In Fig. 11, we have presented the frontier molecule orbital density distributions of the studied compound. Analysis of Fig. 11 shows that the distribution of two energies HOMO and LUMO, we can see that the electron density of the HOMO and LUMO location was distributed almost of the entire molecule.

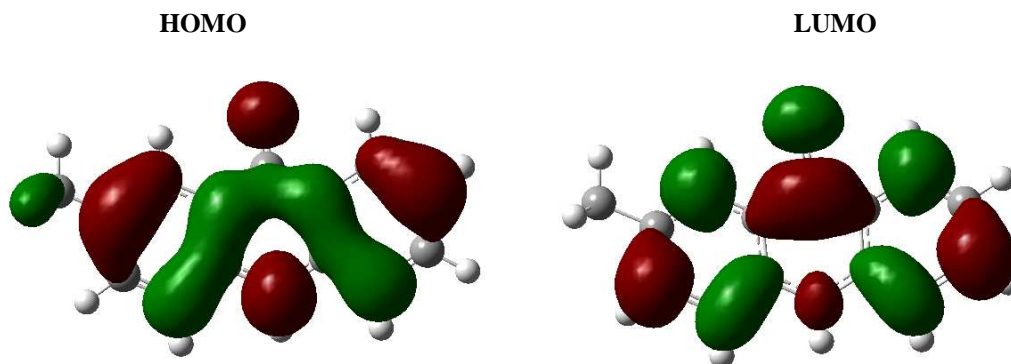


Figure 11. Schematic representation of HOMO and LUMO molecular orbital of studied molecules.

Table 4. Molecular properties of MAO obtained from the optimized structure using DFT at the B3LYP/6-31G\*.

Parameters	MAO
$E_{HOMO}$ (eV)	-5.5167
$E_{LUMO}$ (eV)	-1.4647
$\Delta E_{gap}$ (eV)	4.052
$\mu$ (debye)	4.8438
$I = -E_{HOMO}$ (eV)	5.5167
$A = -E_{LUMO}$ (eV)	1.4647
$\chi = \frac{I + A}{2}$ (eV)	3.4907
$\eta = \frac{I - A}{2}$ (eV)	2.0260
$\sigma = \frac{1}{\eta}$	0.493583
$\Delta N = \frac{\chi_{Fe} - \chi_{inh}}{2(\eta_{Fe} + \eta_{inh})}$	0.86606614
TE (eV)	-18228.04514

According to the frontier molecular orbital theory (FMO) of chemical reactivity, transition of electron is due to interaction between highest occupied molecular orbital (HOMO) and lowest unoccupied molecular orbital (LUMO) of reacting species [80].  $E_{\text{HOMO}}$  is a quantum chemical parameter which is often associated with the electron donating ability of the molecule. High value of  $E_{\text{HOMO}}$  is likely to a tendency of the molecule to donate electrons to appropriate acceptor molecule of low empty molecular orbital energy [81]. The inhibitor does not only donate electron to the unoccupied d orbital of the metal ion but can also accept electron from the d-orbital of the metal leading to the formation of a feedback bond. The highest value of  $E_{\text{HOMO}}$  -5.5167 eV of the studied compound indicates the better inhibition efficiency. On the other hand, it has also been found that an inhibitor does not only donate an electron to the unoccupied d orbital of the metal ion but can also accept electrons from the d orbital of the metal leading to the formation of a feedback bond. Therefore, the tendency for the formation of a feedback bond would depend on the value of  $E_{\text{LUMO}}$ . The lower value of the  $E_{\text{LUMO}} = -1.4647$  eV indicates the easier of the acceptance of electrons from the d orbital of the metal [82,83]. The band gap energy,  $\Delta E = E_{\text{LUMO}} - E_{\text{HOMO}}$  is an important parameter as a function of reactivity of the inhibitor molecule towards the adsorption on metallic surface. As  $\Delta E$  decreases, the reactivity of the molecule increases leading to increase the inhibition efficiency of the molecule. The calculations indicate that our studied molecule has a small value of gap energy (4.052 eV) which means the highest reactivity and accordingly the highest inhibition efficiency which agrees well with the experimental observations. Absolute hardness and softness are important properties to measure the molecular stability and reactivity. It is apparent that the chemical hardness fundamentally signifies the resistance towards the deformation or polarization of the electron cloud of the atoms, ions or molecules under small perturbation of chemical reaction. A hard molecule has a large energy gap and a soft molecule has a small energy gap [84]. In our present work the studied molecule has low hardness value 2.0260 (eV) and a highest value of softness of 0.4939

The most widely used quantity to describe the polarity is the dipole moment of the molecule [85]. Dipole moment is the measure of polarity of a polar covalent bond. It is defined as the product of charge on the atoms and the distance between the two bonded atoms. The total dipole moment, however, reflects only the global polarity of a molecule. For a complete molecule the total molecular dipole moment may be approximated as the vector sum of individual bond dipole moments. The dipole moment ( $\mu$  in Debye) is another important electronic parameter that results from non uniform distribution of charges on the various atoms in the molecule. The high value of dipole moment probably increases the adsorption between chemical compound and metal surface [86]. In our study, the value of the dipole moment is 4.843 debye.

The total energy calculated by quantum chemical methods is equal to -18228.04514 eV. Hohenberg and Kohn [87] proved that the total energy of a system including that of the many body effects of electrons (exchange and correlation) in the presence of static external potential (for example, the atomic nuclei) is a unique functional of the charge density. The minimum value of the total energy functional is the ground state energy of the system. The electronic charge density which yields this minimum is then the exact single particle ground state energy.

## CONCLUSION

- ✓ MAO could acts as an effective corrosion inhibitor for the hydrochloric acid corrosion of steel.
- ✓ MAO is classified as a mixed-type inhibitor.
- ✓ Data obtained from ac impedance technique show a frequency distribution and therefore a modelling element with frequency dispersion behaviour, a constant phase element (CPE) has been used.
- ✓ Application of different isotherms indicated an ideal behavior in the adsorption processes of MAO on the steel surface.
- ✓ The number of active sites occupied by a single inhibitor molecule value indicated that the adsorbed molecules cover four active centers.
- ✓ The inhibition efficiency of the water soluble acridin derivative as corrosion inhibitor indicates that their inhibition effect are closely related to  $E_{\text{HOMO}}$ ,  $E_{\text{LUMO}}$ , hardness, dipole moment and charge densities.

## REFERENCES

- [1] D. M. Strickland, *Ind. Eng. Chem.*, **1923**, 15, 566.
- [2] J. D. Hatfield, A.V. Slack, G. L. Crow, H. B. Shaffer Jr., *J. Agric. Food. Chem.*, **1958**, 6, 524.
- [3] W. Guo, S. Chen, Y. Feng, C. Yang, *J. Phys. Chem. C*, **2007**, 111, 3109.
- [4] S. Lyon, *Nature*, **2004**, 427, 406.
- [5] I.R. Glasgow, A. J. Rostron, G. Thomson, *Corros. Sci.*, **1966**, 6, 469.
- [6] A. K. Singh, M. A. Quraishi, *J. Mater. Environ. Sci.*, **2010**, 1, 101.
- [7] D.D.N. Singh, T.B. Singh, B. Gaur, *Corros. Sci.*, **1995**, 37, 1005.
- [8] M. Prajila, J. Sam, J. Bincy, J. Abraham, *J. Mater. Environ. Sci.*, **2012**, 3, 1045.

- [9] U.J. Naik, V.A. Panchal, A.S. Patel, N.K. Shah, *J. Mater. Environ. Sci.*, **2012**, 3, 935.
- [10] A. Zarrouk, H. Zarrok, R. Salghi, B. Hammouti, F. Bentiss, R. Touir, M. Bouachrine, *J. Mater. Environ. Sci.*, **2013**, 4, 177.
- [11] H. Zarrok, H. Oudda, A. Zarrouk, R. Salghi, B. Hammouti, M. Bouachrine, *Der Pharm. Chem.*, **2011**, 3, 576.
- [12] H. Zarrok, R. Salghi, A. Zarrouk, B. Hammouti, H. Oudda, Lh. Bazzi, L. Bammou, S. S. Al-Deyab, *Der Pharm. Chem.*, **2012**, 4, 407.
- [13] H. Zarrok, S. S. Al-Deyab, A. Zarrouk, R. Salghi, B. Hammouti, H. Oudda, M. Bouachrine, F. Bentiss, *Int. J. Electrochem. Sci.*, **2012**, 7, 4047.
- [14] D. Ben Hmamou, R. Salghi, A. Zarrouk, H. Zarrok, B. Hammouti, S. S. Al-Deyab, M. Bouachrine, A. Chakir, M. Zougagh, *Int. J. Electrochem. Sci.*, **2012**, 7, 5716.
- [15] A. Zarrouk, B. Hammouti, S.S. Al-Deyab, R. Salghi, H. Zarrok, C. Jama, F. Bentiss, *Int. J. Electrochem. Sci.*, **2012**, 7, 5997.
- [16] A. Zarrouk, H. Zarrok, R. Salghi, B. Hammouti, S.S. Al-Deyab, R. Touzani, M. Bouachrine, I. Warad, T. B. Hadda, *Int. J. Electrochem. Sci.*, **2012**, 7, 6353.
- [17] A. Zarrouk, M. Messali, H. Zarrok, R. Salghi, A. Al-Sheikh Ali, B. Hammouti, S. S. Al-Deyab, F. Bentiss, *Int. J. Electrochem. Sci.*, **2012**, 7, 6998.
- [18] H. Zarrok, A. Zarrouk, R. Salghi, Y. Ramli, B. Hammouti, S. S. Al-Deyab, E. M. Essassi, H. Oudda, *Int. J. Electrochem. Sci.*, **2012**, 7, 8958.
- [19] D. Ben Hmamou, R. Salghi, A. Zarrouk, H. Zarrok, S. S. Al-Deyab, O. Benali, B. Hammouti, *Int. J. Electrochem. Sci.*, **2012**, 7, 8988.
- [20] A. Zarrouk, M. Messali, M. R. Aouad, M. Assouag, H. Zarrok, R. Salghi, B. Hammouti, A. Chetouani, *J. Chem. Pharm. Res.*, **2012**, 4, 3427.
- [21] D. Ben Hmamou, M. R. Aouad, R. Salghi, A. Zarrouk, M. Assouag, O. Benali, M. Messali, H. Zarrok, B. Hammouti, *J. Chem. Pharm. Res.*, **2012**, 4, 3489.
- [22] H. Zarrok, H. Oudda, A. El Midaoui, A. Zarrouk, B. Hammouti, M. Ebn Touhami, A. Attayibat, S. Radi, R. Touzani, *Res. Chem. Intermed.*, **2012** DOI 10.1007/s11164-012-0525-x
- [23] A. Zarrouk, B. Hammouti, H. Zarrok, R. Salghi, A. Dafali, Lh. Bazzi, L. Bammou, S. S. Al-Deyab, *Der Pharm. Chem.*, **2012**, 4, 337
- [24] A. Zarrouk, A. Dafali, B. Hammouti, H. Zarrok, S. Boukhris, M. Zertoubi, *Int. J. Electrochem. Sci.*, **2010**, 5, 46.
- [25] A. Zarrouk, T. Chelfi, A. Dafali, B. Hammouti, S.S. Al-Deyab, I. Warad, N. Benchat, M. Zertoubi, *Int. J. Electrochem. Sci.*, **2010**, 5, 696.
- [26] A. Zarrouk, I. Warad, B. Hammouti, A. Dafali, S.S. Al-Deyab, N. Benchat, *Int. J. Electrochem. Sci.*, **2010**, 5, 1516.
- [27] A. Zarrouk, B. Hammouti, R. Touzani, S.S. Al-Deyab, M. Zertoubi, A. Dafali, S. Elkadiri, *Int. J. Electrochem. Sci.*, **2011**, 6, 4939.
- [28] A. Zarrouk, B. Hammouti, H. Zarrok, S.S. Al-Deyab, M. Messali, *Int. J. Electrochem. Sci.*, **2011**, 6, 6261.
- [29] A. Zarrouk, B. Hammouti, A. Dafali, H. Zarrok, R. Touzani, M. Bouachrine, M. Zertoubi, *Res. Chem. Intermed.*, **2011** DOI 10.1007/s11164-011-0444-2
- [30] H. Zarrok, R. Saddik, H. Oudda, B. Hammouti, A. El Midaoui, A. Zarrouk, N. Benchat, M. Ebn Touhami, *Der Pharm. Chem.*, **2011**, 3, 272.
- [31] A. H. Al Hamzi, H. Zarrok, A. Zarrouk, R. Salghi, B. Hammouti, S. S. Al-Deyab, M. Bouachrine, A. Amine, F. Guenoun, *Int. J. Electrochem. Sci.*, **2013**, 8, 2586.
- [32] A. Ghazoui, N. Benaht, S. S. Al-Deyab, A. Zarrouk, B. Hammouti, M. Ramdani, M. Guenbour, *Int. J. Electrochem. Sci.*, **2013**, 8, 2272.
- [33] M. Abdallah, *Corros. Sci.*, **2002**, 44, 717.
- [34] M. A. Hegazy, *Corros. Sci.*, **2009**, 51, 2610.
- [35] R. Hasanov, S. Bilge, S. Bilgic, G. Gece, Z. Kılıc, *Corros. Sci.*, **2010**, 52, 984.
- [36] A. Chetouani, A. Aouniti, B. Hammouti, N. Benchat, T. Benhadda, S. Kertit, *Corros. Sci.*, **2003**, 45, 1675.
- [37] Z. H. Tao, S. T. Zhang, W. H. Li, B. R. Hou, *Corros. Sci.*, **2009**, 51, 2588.
- [38] F. Bentiss, M. Lebrini, H. Vezin, M. Lagrenée, *Mater. Chem. Phys.*, **2004**, 87, 18.
- [39] E. Khamis, *Corrosion*, **1990**, 46, 476.
- [40] E. Stupnisek-Lisac, S. Podbrscek, *J. Appl. Electrochem.*, **1994**, 24, 779.
- [41] E. Stupnisek-Lisac, M. Metikos-Hukovic, *Br. Corros. J.*, **1993**, 28, 74.
- [42] F.B. Growcock, *Corrosion*, **1989**, 45, 1003.
- [43] I. Lukovits, K. Pa'lfı, I. Bako', E. Ka'lma'n, *Corrosion*, **1997**, 53, 915.
- [44] F. Kandemirli, S. Sagdinc, *Corros. Sci.*, **2007**, 49, 2118.
- [45] D. Wang, S. Li, Y. Ying, M. Wang, H. Xiao, Z. Chen, *Corros. Sci.*, **1999**, 41, 1911.
- [46] S.L. Li, Y.G. Wang, S.H. Chen, R. Yu, S.B. Lei, H.Y. Ma, D.X. Liu, *Corros. Sci.*, **1999**, 41, 1769.
- [47] L. Mar'ia Rodr'iguez-Valdez, A. Mart'inez-Villafa'ne, D. Glossman-Mitnik, *J. Mol. Struct.*, **2005**, 713, 65.

- [48] M. Larif, A. Elmidaoui, A. Zarrouk, H. Zarrok, R. Salghi, B. Hammouti, H. Oudda, F. Bentiss, *Res. Chem. Intermed.*, **2011** DOI 10.1007/s11164-012-0788-2.
- [49] A.D. Becke, *J. Chem. Phys.*, **1993**, 98, 5648.
- [50] C. Lee, W. Yang, R.G. Parr, *Phys. Rev. B.*, **1988**, 37, 785.
- [51] B. Miehlich, A. Savin, H. Stoll, H. Preuss, *Chem. Phys. Lett.*, **1989**, 157, 200.
- [52] P.C. Hariharan, J.A. Pople, *Theo. Chim. Acta*, **1973**, 28, 213.
- [53] M.J. Frisch et al., GAUSSIAN 03, Revision B.03, Gaussian, Inc., Wallingford, CT, **2004**.
- [54] W.J. Hehre, L. Radom, P.v.R. Schleyer, A.J. Pople, *Ab Initio Molecular Orbital Theory*, Wiley-Interscience, New York, **1986**.
- [55] J.F. Janak, *Phys. Rev. B.*, **1978**, 18, 7165.
- [56] R. Stowasser, R. Hoffmann, *J. Am. Chem. Soc.*, **1999**, 121, 3414.
- [57] G. Pearson, *Inorg. Chem.* 27 (1988) 734.
- [58] T. Arslan, F. Kandemirli, E.E. Ebenso, I. Love and H. Alemu, *Corros. Sci.*, **2009**, 51, 35.
- [59] K. Jutner, *Electrochim. Acta*, **1990**, 35, 1150.
- [60] T. Paskossy, *J. Electroanal. Chem.*, **1994**, 364, 111.
- [61] M. El. Azhar, B. Mernari, M. Traisnel, F. Bentiss, M. Lagrenee, *Corros. Sci.*, **2001**, 43, 2229.
- [62] A. Yurt, A. Balaban, S.U. Kandemir, G. Bereket, B. Erk, *Mater. Chem. Phys.*, **2004**, 85, 420.
- [63] J.R. Macdonald, W.B. Johnson, in *Theory in Impedance Spectroscopy*, ed. by J.R. Macdonald, Wiley, New York, **1987**.
- [64] E. Mc. Cafferty, N. Hackerman, *J. Electrochem. Soc.*, **1972**, 119, 146.
- [65] N.V. Likhanova, M.A. Dominguez-Aguilar, O. Olivares-Xometl, N. Nava-Entzana, E. Arce, H. Dorantes, *Corros. Sci.*, **2010**, 52, 2088.
- [66] R. Solmaz, *Corros. Sci.*, 52 (2010) 3321.
- [67] Döner, R. Solmaz, M. Özcan, K. Gülfeza, *Corros. Sci.*, **2011**, 53, 2902.
- [68] A. Popova, E. Sokolova, S. Raicheva, M. Christov, *Corros. Sci.*, **2003**, 45, 33.
- [69] I. B. Obot, N. O. Obi-Egbedi, *Corros. Sci.*, **2010**, 52, 198.
- [70] X. H. Li, G. N. Mu, *Appl. Surf. Sci.*, **2005**, 252, 1254.
- [71] I. Langmuir, *J. Am. Chem. Soc.*, **1916**, 38, 2221.
- [72] P. J. Florry, *J. Chem. Phys.*, **1942**, 10, 51.
- [73] M. L. Huggins, *J. Phys. Chem.*, **1942**, 46, 151.
- [74] A.A. El-Awady; B.A. Abd-El-Nabey, S.G. Aziz, *J. Electrochem. Soc.*, **1992**, 19, 2149.
- [75] G. Lyberatos and L. Kobotiatas, *Corrosion*, **1991**, 47, 820.
- [76] R. Solmaz, G. Kardas, M. Culha, B. Yazici, M. Erbil, *Electrochim. Acta.*, **2008**, 53, 5941.
- [77] G. Moretti, F. Guidi, G. Grion, *Corros. Sci.*, **2004**, 46, 387.
- [78] H. Cang, Z. H. Fei, W. Y. Shi and Q. Xu, *Int. J. Electrochem. Sci.*, **2012**, 7, 10121.
- [79] M. Scendo and M. Hepel, *J. Electroanal. Chem.*, **2008**, 613, 35.
- [80] A. Domenicano, I. Hargittai, *Accurate Molecular Structures, Their Determination and Importance*, Oxford University Press, New York, **1992**.
- [81] M. J. S. Dewar, W. Thiel, *J. Am. Chem. Soc.*, **1977**, 99, 4899.
- [82] A.Y. Musa, A. H. Kadhum, A. B. Mohamad, A.b. Rohoma, H. Mesmari, *J. Mol. Struct.*, **2010**, 969, 233.
- [83] M.A. Amin, K.F. Khaled, S.A. Fadel-Allah, *Corros. Sci.*, **2010**, 52, 140.
- [84] G. Gece, S. Bilgic, *Corros. Sci.*, **2009**, 51, 1876.
- [85] O. Kikuchi, *Quant. Struct.-Act. Relat.*, **1987**, 6, 179
- [86] E.E. Ebenso, D.A. Isabirye, N.O. Eddy, *Int. J. Mol. Sci.*, **2010**, 11, 2473.
- [87] H. Ju, Z.P. Kai, Y. Li, *Corros. Sci.*, **2008**, 50, 865.